Detection of *E.coli* 23S rRNA by electrocatalytic "off-on" DNA beacon assay with femtomolar sensitivity

Rimsha B. Jamal [a], Toni Vitasovic [a], Ulrich Gosewinkel [b], Elena E. Ferapontova [a,*]

[a] *Interdisciplinary Nanoscience Center (iNANO) and Aarhus University Center for Water Technology (WATEC), Faculty of Science, Aarhus University, Gustav Wieds Vej 14, 8000, Aarhus C, Denmark*
[b] *Department of Environmental Science, Aarhus University, Frederiksborgvej 399, DK-4000, Roskilde, Denmark*

A B S T R A C T

Prevention of food spoilage, environmental bio-contamination, and pathogenic infections requires rapid and sensitive bacterial detection systems. Among microbial communities, the bacterial strain of *Escherichia coli* is most widespread, with pathogenic and non-pathogenic strains being biomarkers of bacterial contamination. Here, we have developed a fM-sensitive, simple, and robust electrocatalytically-amplified assay facilitating specific detection of *E.coli* 23S ribosomal rRNA, in the total RNA sample, after its site-specific cleavage by RNase H enzyme. Gold screen-printed electrodes (SPE) were electrochemically pre-treated to be productively modified with a methylene-blue (MB) – labelled hairpin DNA probes, which hybridization with the *E. coli*-specific DNA placed MB in the top region of the DNA duplex. The formed duplex acted as an electrical wire, mediating electron transfer from the gold electrode to the DNA-intercalated MB, and further to ferricyanide in solution, enabling its electrocatalytic reduction otherwise impeded on the hairpin-modified SPEs. The assay facilitated 20 min 1 fM detection of both synthetic *E. coli* DNA and 23S rRNA isolated from *E.coli* (equivalent to 15 CFU mL^{-1}), and can be extended to fM analysis of nucleic acids isolated from any other bacteria.

1. Introduction

Worldwide 1 out of 10 people fall ill each year due to bacterial contamination in food, which makes up a total population of 600 million, and approximately 420 000 people die, with one-third of them being children. Such outbreaks pose not only a serious threat to human health but also bring an economic burden of 110 billion US dollars each year due to hospitalizations and product re-runs (WHO report 2019). With a rapidly developing market of minimally processed food and ready-to-eat products, such outbreaks are likely to happen more frequently. Among pathogenic bacterium causing such outbreaks, the bacterial strain of *E.coli* is most common, with 10 *E.coli* CFU mL^{-1} in dairy products (Grade A Pasteurized Milk Ordinance, 2017), and one *E. coli* in 100 mL of drinkable water (WHO, 1997) causing illness. Timely detection of bacterial contamination thus requires fast, specific and sensitive, yet simple approaches for bacterial analysis; with electrochemical assays providing one of the best sensitivities and speed of analysis (Campuzano et al., 2017; Ferapontova, 2017a; Jamal et al., 2020; Kirsch et al., 2013).

Among those is electrochemical sensing of bacterial DNA or RNA through their hybridization on electrodes, exploiting differences in electrochemistry of single stranded (ss) and double stranded (ds) DNA (Ferapontova, 2017b; Palecek and Bartosik, 2012). It allows designing electrochemical hybridization assays exploiting synthetic, chemically-modified probe DNA sequences, such as bearing redox-active labels that interact differently with both structures, ss and dsDNA (Ferapontova, 2020). Redox probes can intercalate into dsDNA and produce an electrochemical response due to their redox transformation mediated by the DNA duplex, transferring electrons from the electrode to the redox probe. Such DNA-mediated electron transfer (ET) through the π-stack of nucleobases is exceptionally sensitive to any perturbations induced by mutations, at a single-nucleotide polymorphism (SNP) level (Campos et al. 2014, 2018; Kelley et al., 1999), and was intensively used in hybridization assays for SNP detection in cancer diagnostic applications (Boon et al., 2000; Hartwich et al., 1999; Slinker et al., 2011). However, the sensitivity of such detection platforms is either restricted to solely SNP detection (DNA hybridization is performed in solution and thus DNA is not quantified) (Boon et al., 2000; Slinker et al., 2011) or challenged at concentrations <0.5 μM SNP DNA (Jiang et al., 2005), due to the insignificant 1–6 °C difference in T_m of the SNP-containing and

fully complimentary duplexes when a linear DNA probe is used. Alternatively, a hairpin DNA probe consisting of a self-complementary stem and a target-recognizing loop provides a T_m difference of 10–14 °C (Abi and Ferapontova, 2013). The larger difference in T_m results in less stable SNP-containing duplexes, which increases assay's hybridization specificity at the SNP level (Bonnet et al., 1999).

In the simplest assay, the redox-labelled hairpin DNA structure is immobilized through the alkanethiol linker on gold electrodes, while another end of the hairpin is redox labelled. DNA hybridization moves the redox label away from the electrode surface, which alters the ET distance, and provides distinctly different signals from ssDNA and dsDNA, with a limit-of-detection (LOD) of 10 pM DNA when ferrocene was used as a redox label (Fan et al., 2003) and 200 nM DNA - with methylene blue (MB) (Lubin et al., 2006). A major drawback of such assays is a decreasing analytical "on-off" response, which can result in false positives when DNA is desorbed. Target-induced strand displacement, bringing the MB label closer to the electrode surface and increasing the ET rate (Xiao et al., 2006), enzymatic labels for signal amplification triggered upon hybridization (Liu et al., 2008), or a triple-loop probe structures in which hybridization released a flexible, MB-labelled single-strand segment enabling enhanced direct ET between the label and the electrode surface (Xiao et al., 2009) allowed signal "off-on" assays. In the simplest "off-on" approach, a truncated hairpin beacon labelled with charged MB allowed the diffusion-limited ET of MB in a hybrid and, as a result, the "off-on" signal change and nM DNA detection (Farjami et al., 2011). In all these approaches, the SNP sensitivity was only partially addressed (Farjami et al., 2011), and, at its best, pM levels of DNA were detected (Kékedy-Nagy et al., 2018).

In this work, we have developed a simple yet fast and sensitive electrocatalytic assay for bacterial RNA, exploiting DNA and rRNA hybridization to the hairpin DNA probe, immobilized on the gold screen-printed electrode (Au SPE) surface, and DNA-mediated electrocatalysis for signal amplification. DNA-mediated electrocatalysis proceeding in compact dsDNA self-assembled monolayers (SAM), with dsDNA-intercalated MB operating as an electrocatalytic center for ferricyanide reduction, is a well-known way to enhance the sensitivity of SNP detection (Furst et al. 2014, 2019). In such assays, hybridization of thiolated DNA probes with target DNA is performed in solution, and then the formed duplexes are immobilized densely on gold electrodes, where DNA-intercalated MB electrocatalyzes reduction of ferricyanide, whose electrochemistry is otherwise impeded on the formed compact negatively-charged DNA SAM (Kelley et al., 1999). No quantification of target DNA however is possible in such assays, but only the SNP detection.

Nevertheless, such electrocatalytic platform is very attractive for the development of hybridization sensors with improved sensitivity and low LOD. A crucial element in such assays is design of the DNA|electrode interface capable both of productive hybridization and of the electrocatalytic response exclusively. For this, the DNA surface coverage (Γ_{DNA}) should be kept above 2.2 but below 5 pmol cm^{-2}, in order (a) to block the surface against the direct ferricyanide discharge (Kékedy-Nagy and Ferapontova, 2019) and (b) to be still sufficiently low for structurally unimpeded hybridization (Kékedy-Nagy et al., 2018).

In our approach, to ensure predictable and stable reference signals that are independent of the DNA probe sequence and length (Kékedy-Nagy et al., 2018), we immobilized on gold conformationally rigid, MB-labelled hairpin DNA probes (Abi and Ferapontova, 2013; Xiao et al., 2007a), with this forming the DNA SAM capable of electrocatalytic quantification of target DNA. To adapt the assay for rapid on-site testing, we used Au SPE facilitating easy translation of lab-developed assays to in-field diagnostic setups. The compact structure of a three-electrode system on a single ceramic chip allows detection in 80 μL sample volumes, making it perfectly suitable for remote detection. However, the quality of the Au SPE surface was insufficient for proper assembling of DNA and formation of SAM with required properties (NB: such SPE are rather routinely used as a substrate for gold deposition and then for assay development (Ingrosso et al., 2019; Khater et al., 2019; Liu et al., 2012). Thus, we have developed the protocol for Au SPE pre-treatment providing Au surface suitable for immobilization of the DNA probe capable of biorecognition of the target nucleic acid sequences and the electrocatalytic operation of the genosensor. The assay was used for specific detection of 23S ribosomal rRNA extracted from *E.coli*.

2. Materials and methods

Materials. All DNA sequences used in this work were ordered from Metabion Int. AG, (Planegg, Germany) and are presented in Table 1. For site-specific cleavage of *E.coli* 23S rRNA with RNase H enzyme, 15-mer 5′- ACA CTG GGT TTC CCC -3′ complementary DNA sequence before (P1) and 23-mer 5′ - CGC CTC ATT AAC CTA TGG ATT CA -3′ complementary DNA sequence after (P2) the probe specific region were used. Freeze-dried *E.coli* DH5α (DSM's strain no.6897) and *Bacillus subtilis* cells (DSM's strain no.10) were supplied by DSMZ (Braunschweig, Germany). *Pseudomonas fluorescens* strain F113^T (a.k.a. *Pseudomonas ogarae* (Garrido-Sanz et al., 2021), DSM's strain 112162^T) was from the library of the Department of Environmental Science, Aarhus University, Roskilde, Denmark.

Bacterial rRNA isolation. *E. coli* was grown in 2 L of Luria-Bertani (LB) broth at 37 °C for 18 h under shaking at 120 rpm in a shaking incubator Innova 4000 Shaker (New Brunswick Scientific, UK). The overnight culture was then centrifuged for 5 min at 5000 rpm using Eppendorf Mini Spin 5452 centrifuge (Eppendorf AG, Germany), at room temperature (rt). The supernatant was discarded, and the resulting pellets were washed in a sterile 20 mM PB/150 mM NaCl buffer (pH 7.0), followed by centrifugation at 5000 rpm for 5 min. The supernatant was discarded, and the washing was repeated one more time with centrifugation as before. The final pellet was re-suspended in 1 mL sterile 20 mM PB/150 mm NaCl buffer (pH 7.0). Finally, the concentration of re-suspended bacteria was estimated by optical density (OD) measurements at 600 nm using UV Mini-1240 UV-VIS spectrophotometer (Shimadzu Co., Japan), with the conversion factor of OD_{600} (1.0) = 5×10^8 cells mL^{-1}. *E. coli* rRNA was extracted using the NucleoSpin RNA Plus kit (Machery-Nagel, Duren, Germany) according to the manufacturer protocol (**SI**). The rRNA purity and concentration was determined using the DeNovix DS-11 spectrophotometer, Wilmington, USA, using a 1 μL sample. The total rRNA sample showed absorbance ratios $A_{260/280}$ of 2.026 and $A_{260/230}$ of 1.204. Two other bacterial strains were grown for 24 h at 30 °C, the rest procedures being the same as for *E.coli*; their rRNA was extracted using practically the same protocol (**SI**).

***E.coli* rRNA sample pre-treatment.** Prior detection, extracted total rRNA was treated with RNase H enzyme to cut out a 22 nts sequence complementary to the *E.coli* detection probe from 2904 nts long 23S

Table 1
Thiolated and MB-labelled DNA sequences used in this work.

Name of the sequence	Composition
20-mer TP53-specific hairpin probe	5′- MB-GTT GTG CAG CGC CTC ACA AC-thiol-C6-3′
20-mer TP53 target (short PM-cDNA)	5′- GTT GTG AGG CGC TGC ACA AC-3′
28-mer TP53 target (long PM-cDNA)	5′-GAG GTT GTG AGG CGC TGC CCC CAC CAT G-3′
20-mer TP53 target with SNP (short SNP-cDNA)	5′- GTT GTG AGG CAC TGC ACA AC-3′
28-mer TP53 target with SNP (long SNP-cDNA)	5′-GAG GTT GTG AGG CAC TGC CCC CAC CAT G-3′
28-mer *E.coli* 23S rRNA-specific hairpin probe	5′-Thiol-C6-GTT AAT GAT AGT GTG TCG AAA CAT TAA C- MB-3′
27-mer *E.coli* 23S rRNA-specific hairpin probe	5′-Atto MB2-GTT TCG TTA ATG ATA GTG TGT CGA AAC-Thiol-C6-3′
22-mer *E.coli* 23S rRNA-specific target	5′-GTT TCG ACA CAC TAT CAT TAA C-3′

rRNA, as it specifically recognizes and cleaves the phosphodiester of an RNA strand in a DNA/RNA hybrid while leaving the RNA strand intact. For this purpose, 5 μL of 10 μM P1 and 5 μL of 10 μM P2 and 6 μL of 50 mM PB/150 mM NaCl were added to 34 μL of extracted rRNA, giving a final volume of 50 μL; after 5 min hybridization at 90 °C, the sample was cooled for 5 min in a water bath at rt. 1 μL (5 units) of RNase H enzyme (M0523S, Newengland BioLabs, Hitchin, UK), 10 μL of the provided reaction buffer (Tris buffered with HCl: 7.9%, KCl: 5.6%, and dithio-threitol (DTT): 1.5%) and 39 μL nuclease-free water were then added to the sample giving a total volume of 100 μL. The mixture was incubated at 50 °C for 20 min, followed by the addition of 1 μL of 0.5 M EDTA to stop the enzymatic reaction. This final mixture containing cleaved 22 nts-long *E.coli*-specific 23s rRNA sequence was analyzed as digested *E. coli* rRNA. Samples of total rRNA extracted from *B. subtilis* and *P. fluorescens* cells were similarly treated with P1/P2 and the enzyme (**SI**).

Electrode Pre-treatment. Gold screen-printed electrodes (Au SPE, DRP-220BT, DropSens, Metrohm, Denmark) incorporated gold working and counter electrodes (WE and CE, WE's $A_{geom} = 0.1256$ cm^2) and a silver pseudo-reference electrode (RE). Au SPE were carefully washed with Milli-Q water and a 100 μL drop of 0.5 M H$_2$SO$_4$ was placed on the SPE surface covering all electrodes. In total 22 cyclic voltammetry scans (6-10-6, with a Milli-Q water washing in-between) were run within the −0.2 -+1.2 V potential window, at a scan rate 0.1 V s^{-1} (Malecka et al., 2016). The electrochemical surface area of WEs was estimated by inte-grating Au surface oxide reduction CV peaks in 0.1 M H$_2$SO$_4$ at 0.3 V s^{-1} (a conversion factor: 390 μC cm^{-2}) (Trasatti and Petrii, 1992).

Electrode modification with probe DNA. For duplex immobilization, a freshly prepared mixture of 2.6 μM thiol-modified DNA (probe), 3.9 μM cDNA (target), and 6.76 mM TCEP were left for 1 h at rt in the dark and humid environment, for disulfide bond reduction. Then, 50 mM PB/ 150 mM M NaCl/20 mM MgCl$_2$, pH 7 (immobilization buffer) was added, and 9 μL of this solution with final concentrations of 2 μM probe, 3 μM target, and 5 mM TCEP were placed on the WE surface. The modified WE electrode was rinsed with 20 mM PB/150 mM NaCl, pH 7 (PBS), and exposed to 9 μL of 2 mM MC$_6$OH (prepared in the same buffer) for 1 h 40 min at RT. After washing in PBS, the dsDNA-modified electrodes were immediately used in experiments. For ssDNA probe immobilization, a mixture of 1 μM thiol-modified DNA (probe) and 0.05 mM TCEP in 50 mM PB/150 mM NaCl, pH 7, was left for 1 h at rt for disulfide bond reduction, and a 9 μL drop of this mixture was immedi-ately placed onto the WE surface and left for 12 h at rt, in the dark and humid environment. The ssDNA-modified WE electrode was rinsed with PBS, and exposed to 9 μL of 10 mM MC$_6$OH (prepared in the same buffer) for 30 min. Following washing with PBS, these electrodes were imme-diately used in experiments.

Electrochemical measurements. Cyclic voltammetry (CV) and chronocoulometry (CC) measurements were performed with a μAutolab potentiostat (Type III, Metrohm, Utrecht, Netherlands) equipped with GPES software (version 4.9.007), inside a faradaic cage, in dark, at rt. When not stated otherwise, the measurements were performed in a 3 mL cell with an external Ag/AgCl (3M KCl) RE. Non-catalytic CVs were recorded in PBS, while electrocatalytic CVs and CC were recorded in 20 mM PB, pH 7, containing 0.2 mM K$_3$[Fe(CN)$_6$]. In CC, the −400 mV potential was applied for 10 s. After the DNA or RNA sample addition and 20 min hybridization under constant magnet stirring, the CV and CC measurements were performed in quiet solutions.

3. Results and discussion

DNA immobilization on Au SPE. In biosensor research, Au SPE are typically used as a substrate for gold electrodeposition and further DNA immobilization (Khater et al., 2019; Liu et al., 2012), and just a few works that use Au SPE for immediate immobilization of DNA report a quite low DNA surface coverage, Γ_{DNA}, from 0.08 to 1.6 pmol cm^{-2} (Rossetti et al., 2020). At its higher limit, this Γ_{DNA} is less than 20% of

the theoretical limiting Γ_{dsDNA}, of ca. 8.6 pmol cm^{-2} (Hartwich et al., 1999), which is also essentially lower than Γ_{DNA} obtained at gold disk electrodes (Farjami et al., 2011; Kékedy-Nagy et al., 2016). Most important, for efficient MB-mediated electrocatalysis of ferricyanide reduction, Γ_{DNA} should exceed 2.2 pmol cm^{-2}; such Γ_{DNA} preventing direct discharge of ferricyanide on the DNA-free electrode surface (Kékedy-Nagy and Ferapontova, 2019; Kékedy-Nagy et al., 2019).

Thus, first, we interrogated the efficiency of the Au SPE modification with thiolated DNA probes and the quality of the formed DNA SAM. In these experiments, we used a well-studied ssDNA hairpin beacon/ dsDNA system designed in our group (Farjami et al., 2011; Kékedy-Nagy et al. 2016, 2018) (Table 1). Thiolated, 20-mer TP53-gene-specific hairpin probe sequence was 5′-labelled with MB, which, in contrast to our earlier work (Farjami et al., 2011), did not bear extra negatively-charged COOH functionality and, thus, was able to interca-late into dsDNA after hybrid formation (Kékedy-Nagy et al., 2016).

Hybridization and conformational changes in this hairpin probe and duplexes it forms were confirmed by quartz crystal microbalance (QCM-D) studies, performed directly on the surface of gold chips (Papadakis et al., 2012). Such probes and their hybrids could be easily regenerated on the electrode surface by a simple, rt rinse with Milli-Q water (Lai et al., 2006; Lubin et al., 2006; Xiao et al. 2007a, 2007b), the melting temperature, T_m, of the probe of 43.7 °C and that of the hybrid of 59.8 °C (in the 20 mM PB solution) fitting both requirements of probe hybrid-izability and water-regeneration.

Immobilization of ssDNA on un-pretreated Au SPE (for 12 h), ac-cording to the protocol earlier developed for Au disk electrodes (Farjami et al., 2011; Kékedy-Nagy et al., 2018), did not yield DNA SAM pro-ductive for hybridization (Fig. 1A). Though Γ_{DNA} of 2.9 ± 0.5 pmol cm^{-2} was sufficiently high, no essential changes in the MB signal after hy-bridization was seen. Electrode washing with Milli-Q water resulted in decreasing CV peak currents correlating rather with the DNA surface loss due to non-specific adsorption/desorption than with expected de-hybridization (Lubin et al., 2006; Xiao et al., 2007a). To overcome non-specific binding of ssDNA to gold via nucleobases (Campos et al., 2018; Piana and Bilic, 2006), a 1 h dsDNA immobilization (Boon et al., 2003) followed by de-hybridization was probed. Such immobilization usually results in densely packed DNA SAMs on clean gold surfaces (Boon et al., 2000). However, despite the obtained high Γ_{DNA} of 5.1 ± 0.3 pmol cm^{-2}, MB signals from dsDNA and hairpin ssDNA, presumably formed after dsDNA de-hybridization in Milli-Q water, differed insig-nificantly (Fig. 1C), again indicating some non-specific binding of DNA to the Au SPE surface, not via the thiol linker.

Thiol-gold bond formation requires activated, clean gold surface, and it was clear that the quality of the Au SPE surface was insufficient, and needed electrochemical pre-treatment, such as routinely used with conventional Au disk electrodes (Ferapontova and Gothelf, 2009). ssDNA immobilized on such electrochemically pre-treated Au SPE gave a higher Γ_{DNA} of 5.7 ± 0.7 pmol cm^{-2} indeed. However, the latter was associated rather with enhanced non-specific adsorption of ssDNA via nucleobases on the activated Au surface (Fig. 1B), since the voltammetrc signals from MB did not significantly change neither after hybridization nor after de-hybridization. Thus, 12 h adsorption of ssDNA on the activated Au SPE resulted in the formation of non-hybridizable SAM. Shorter immobilization times (from 1 to 2 h) yielded $\Gamma_{DNA} < 2.2$ pmol cm^{-2}, consistent with previous reports (Rossetti et al., 2020).

Finally, dsDNA was immobilized onto the activated Au SPE, and only this approach resulted in the formation of DNA SAMs responding to de- and re-hybridization and displaying a classical electrochemical beacon behavior (Lai et al., 2006; Xiao et al., 2007a). Analysis of electro-chemical signals allowed mechanistic discrimination between the interfacial states of dsDNA and ssDNA (Fig. 1D). Generally, lower signals and a wider peak separation are characteristic of a slower ET reaction, while increased signals and smaller peak separations, after the de-hybridization, are consistent with a faster ET reaction (Laviron, 1979). Indeed, MB-labelled dsDNA SAMs showed characteristic CV
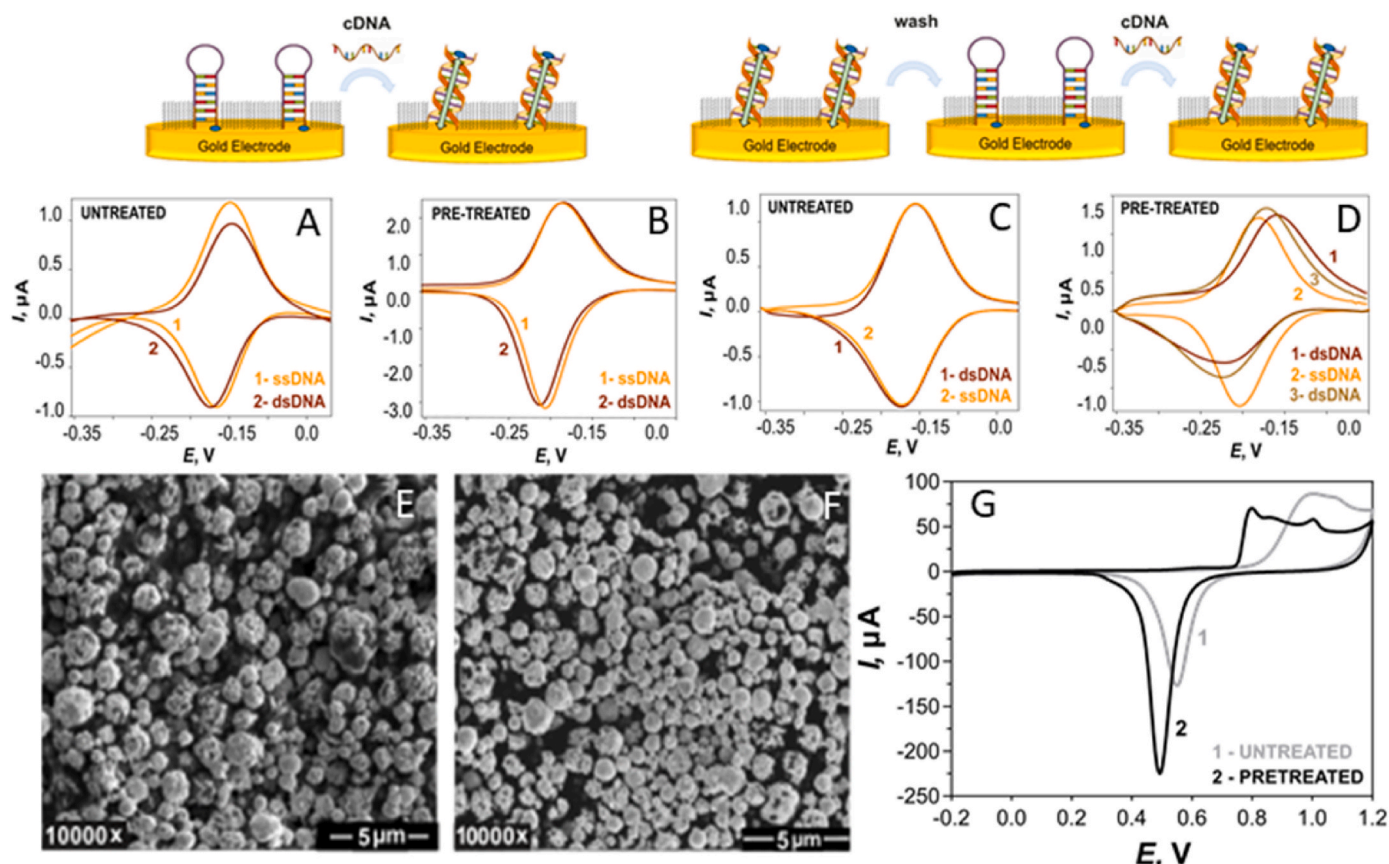
Fig. 1. Top: schematic presentation of ssDNA and duplex immobilization strategies; (A–D) representative background-corrected CVs recorded in 20 mM PB/150 mM NaCl with Au SPE (A, B) modified with ssDNA, (A) un-pretreated SPE, $\Gamma_{MB} = 2.9 \pm 0.5$ pmol cm^{-2} (B) electrochemically pre-treated, $\Gamma_{MB} = 5.7 \pm 0.7$ pmol cm^{-2} (C, D) modified with dsDNA, (C) un-pretreated, $\Gamma_{MB} = 5.1 \pm 0.3$ pmol cm^{-2}, and (D) electrochemically pre-treated, $\Gamma_{MB} = 3.2 \pm 0.4$ pmol cm^{-2}. Scan rate: 1 V s^{-1}. (E, F) Representative SEM images of (E) Au SPE as delivered and (F) electrochemically pre-treated by cycling in 0.5 M H$_2$SO$_4$. SEM scale bar: 5 μm. (G) Representative CVs of Au SPE oxidation/reduction recorded in 100 μl of 0.1 M H$_2$SO$_4$. Scan rate: 0.1 V s^{-1}.

peaks of MB, with a peak separation ΔE_p of 67 ± 2 mV due to the long-range ET mediated by the duplex, from the electrode to DNA-intercalated MB (Kelley et al., 1999; Slinker et al., 2011) (Fig. 1D). Upon DNA de-hybridization in Milli-Q water, ΔE_p decreased to 16 ± 4 mV, consistent with the enhanced ET between the electrode and MB in the folded hairpin DNA placing MB in proximity to the electrode surface (Abi and Ferapontova, 2013). Upon re-hybridization, MB signals returned to the original, dsDNA-characteristic shape. We could conclude that DNA duplexes then were immobilized on Au SPE via the alkanethiol linker and capable of de-hybridization, while then generated hairpin ssDNA probes were capable of re-hybridization. Therewith, the obtained Γ_{DNA} of 3.2 ± 0.4 pmol cm^{-2} was sufficiently dense for successful electrocatalytic sensing.

Thus, electrochemical cleaning of Au SPE electrodes was crucial for proper immobilization of DNA via the thiol linker, avoiding non-specific DNA binding. Both CV and SEM imaging revealed the partial reconstruction of the electrode surface after electrochemical cleaning (Fig. 1E–G), with then displayed energetically-distinct well-defined crystallographic facets characteristic of clean gold (seen in the oxidation peak) and general topography of the surface tending to smaller and more evenly packed gold micro- and sub-microclusters. Due to restructuring, the real surface area of electrochemically pre-treated SPEs, determined by integrating gold surface reduction peaks (Fig. 1G), increased from 0.124 cm^2 of original Au SPE to 0.197 cm^2 (the roughness factor increase from 1 to 1.6).

Electrocatalytic genosensor using TP53-specific hairpin DNA probe as a model. A TP53-specific 20 nts hairpin probe, MB-labelled, was immobilized on the electrochemically activated Au SPE in the 20-mer

duplex form and further re-hybridized. Electrocatalysis of ferricyanide reduction mediated by MB, intercalated either in the top region of dsDNA or in the stem of the hairpin ssDNA probe, was evaluated by CV. Negligible currents of ferricyanide reduction were observed at ssDNA-modified electrodes, in which MB was buried inside the ssDNA SAM sterically hindering its ability to reduce ferricyanide (Fig. 2A(1), B(1)). Such hairpin construction provided a robust and minimized background signal. Hybridization, placing MB in the top of the SAM, resulted in the electrocatalytic 20-fold enhancement of the current response (at -0.35 V, **Figure A(2), B(2)**). The presence of SNP in the duplex then, as expected, decreased the signal intensity 5-fold, consistent with a lower-efficient DNA-mediated ET along the SNP-containing duplex, due to its high sensitivity to the minor disturbance of the DNA base-pair π-stack (Boon et al., 2000; Campos et al., 2014) **(Figures A(3), B(3))**. Thus, we formed the DNA SAM on Au SPE that enabled switching between the hybridizable hairpin ssDNA probe and the on-surface hybridized duplexes yielding enhanced electrocatalytic signals that was further calibrated versus the concentration of the analyzed cDNA.

To detect cDNA more sensitively and in a more robust way than the dynamic CV technique, constant potential chronocoulometry, CC, shown to be advantageous for measuring signals from electrocatalytic processes (Boon et al., 2000; Díaz-Fernández and Ferapontova, 2022; Gómez-Arconada et al., 2022; Malecka and Ferapontova, 2021), was used for DNA hybridization detection (Fig. 2C, S1). In our case, the CC responses may be generally correlated with the total charge Q passing through the system (Anson, 1966):

$$Q = (2nFAD_{K3[Fe(CN)6]}^{1/2} C_{K3[Fe(CN)6]} * t^{1/2})/\pi^{1/2} + Q_{EDL} + Q_{MB}, \qquad (1)$$
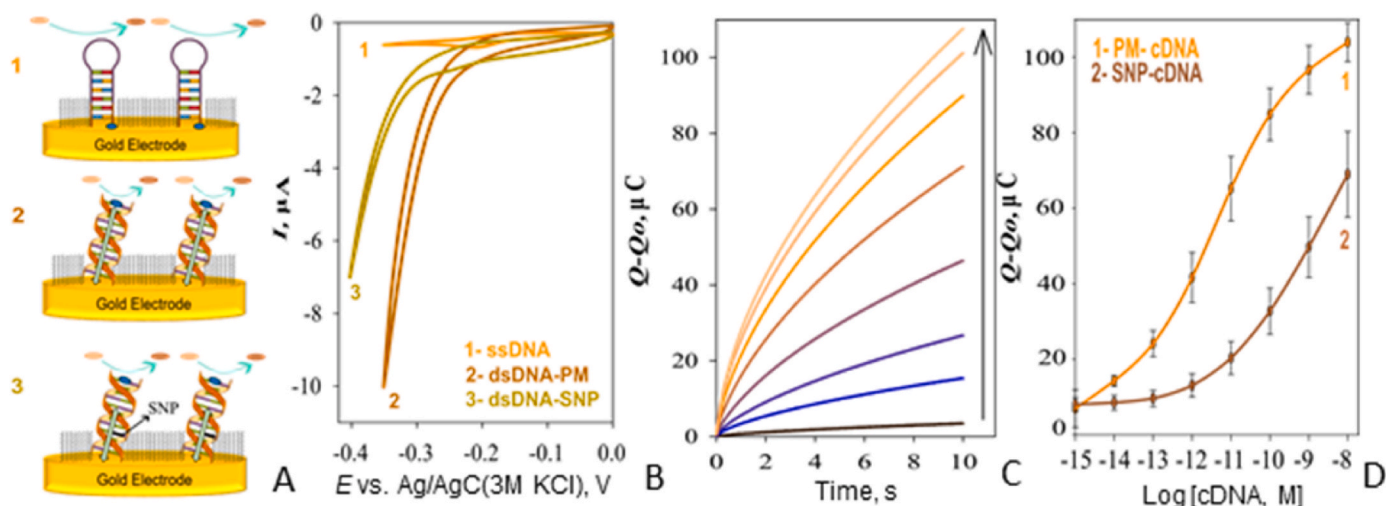
Fig. 2. (A) Schematic of the interfacial design of the electrodes modified with MB-labelled 20 nts TP53-specific (1) ssDNA and (2, 3) dsDNA, (2) perfectly matched and (3) SNP-containing, and (B) representative CVs recorded with these electrodes in 20 mM PB/150 mM NaCl/0.2 mM $K_3[Fe(CN)_6]$. Scan rate: 0.5 Vs^{-1}. PM-cDNA: $\Gamma_{MB} = 2.6 \pm 2.0$ pmol cm^{-2}; SNP-cDNA: $\Gamma_{MB} = 2.8 \pm 0.2$ pmol cm^{-2}. (C) Representative chronocoulometry (CC) data recorded with Au SPE modified with ssDNA at -0.4 V and 10 s sampling time in 20 mM PB/0.2 mM $K_3[Fe(CN)_6]$, in the presence of increasing concentrations of PM-cDNA as indicated by arrow: 1, 10, 100 fM, 1, 10, 100 pM, 1 and 10 nM. (D) Calibration curves for (1) PM-cDNA and (2) SNP-cDNA detection constructed with CC data (10 s polarization time).

once the ability of MB to electrocatalytically reduce ferricyanide is kept constant. Here, $D_{K3[Fe(CN)6]}$ is the diffusion coefficient (in cm^2 s^{-1}) and $C_{K3[Fe(CN)6]}^*$ is the concentration of ferricyanide (in mol cm^{-3}). With increasing polarization time t the charge associated with the electrocatalytic reduction of ferricyanide (the first summand in Eq. (1)) accumulates, starting to dominate over both the contribution from the electric double layer charging Q_{EDL} and the charge associated with the redox transformation of MB, Q_{MB}.

Hybridization of the hairpin probe with a perfectly-matched similar-length cDNA led to the increasing CC responses starting from 1 fM cDNA. Calibration curves associated with the CC responses of ssDNA-modified Au SPE to hybridization were constructed by plotting the Q-Q_0 changes (Q_0 is a background CC signal from the folded hairpin probes, curve 1 in Fig. 2B) collected at different polarization potentials of -0.25, -0.30, -0.35, and -0.40 V against the logarithmic cDNA concentration (Fig. 2D, S2). The CC response increased with increasing concentrations of cDNA up to 10 nM, with the highest sensitivity of 200 µC cm^{-2} M^{-1} (a slope of the linear part of calibration curves) detected at -0.4 V, and LOD of 1 fM, defined by the IUPAC as "*the smallest amount of concentration of analyte in the sample that can be reliably distinguished from zero*". This LOD was identical to LOD evaluated as a cDNA concentration equivalent to the blank solution signal summed 3 times its standard deviation. It was essentially, several orders of magnitude lower than LODs shown with other redox-labelled hairpin beacons in the absence of electrocatalysis (Fan et al., 2003; Farjami et al., 2011; Kékedy-Nagy et al., 2016; Ricci et al., 2007), and improved 4 orders of magnitude compared to 10 pM LOD shown for the same beacon system with MB as a soluble redox indicator (Kékedy-Nagy et al., 2018).

The observed "off-on" signal response of the designed electrocatalytic genosensor to cDNA binding favorably contrasts with basic sensing platforms exploiting redox-labelled hairpin probes and hybridization-associated changes in the ET efficiency (Fan et al., 2003; Farjami et al. 2011, 2012; Lai et al., 2006). This LOD is comparable with the best fM LOD examples exploiting ferricyanide as a redox indicator and unlabeled hairpin probes (Kjällman et al., 2008; Koo et al., 2016). Along with that, the suggested assay not only addresses analysis of non-amplified samples but also shows the selectivity for SNP and can be further elaborated for analysis of mutated DNA/microRNA in cancer diagnostics (Ferapontova, 2017b, 2017c; Furst et al., 2019). Therewith, by using the hairpin design of the probes, as opposed to the flexible linear probes that can place the redox label at an arbitrary distance

relative the electrode surface, we obtained a manageable background signal not compromised by the variety of possible linear DNA probe structures (Kékedy-Nagy et al., 2018), thus warranting the robust "off-on" signal change.

The sensitivity of the DNA-mediated long-range ET for SNP allowed discrimination between the perfectly matched and SNP-containing cDNAs, with the largest difference in responses (5 - 3 fold) observed within the 1 fM – 0.1 nM range (Fig. 2D). At higher concentrations, the saturation plateau observed for the perfectly matched target restricted sensor's SNP discrimination ability. It is also interesting, that within the 1–100 fM range, SNP-containing cDNA produced the "background" (not calibrated) signal equivalent to the response from 1 fM perfectly-matched cDNA, with the most productive detection range being between 10 fM and 0.1 nM. While in cancer diagnostics, due to the inherently low concentrations of, e.g., cancer-related microRNA in physiological fluids, such sensor could provide useful information about dis-regulation of structurally close microRNA sequences (Kékedy-Nagy et al., 2018), this feature is less important in bacterial analysis of rRNA regions highly specific for particular species. It is worth to mention that the highest sensitivity of DNA detection was at -0.4 V, while -0.35 V provided the highest sensitivity for SNP (Fig. S3). Aiming at bacterial rRNA detection, we focused on the conditions that allowed the most sensitive detection of DNA.

Electrocatalytic detection of cDNA exceeding the length of the hairpin probe. We have developed a successful electrocatalytic system composed of two DNA strands, the hairpin probe and cDNA, of the same length, which is far from the real world situation. Practically, in any hairpin-beacon structure designed for analysis of real world DNA/RNA samples, there always will be a non-complementary region at the top of the formed duplex, representing the part of a hairpin stem bearing the redox probe (Abi and Ferapontova, 2013; Xiao et al., 2007a). It was unclear, how productively in this case can the MB label intercalate into the duplex to ensure efficient DNA-mediated ET and electrocatalysis for DNA detection (Fig. 3A). Indeed, hybridization of the 20 nts hairpin beacon to the TP53-specfic 28 nts long cDNA (Farjami et al., 2011) resulted in the formation of dsDNA having at its top two non-complementary regions: the MB-bearing 5 nts overhang (the stem region of the probe) and 13 nts overhang from the cDNA. The response from such hybrid was less pronounced compared to the fully complementary 20 nts long cDNA, though the sensitivity of cDNA detection appeared the same (Fig. 3B and C). Overall, the intensity of the signals
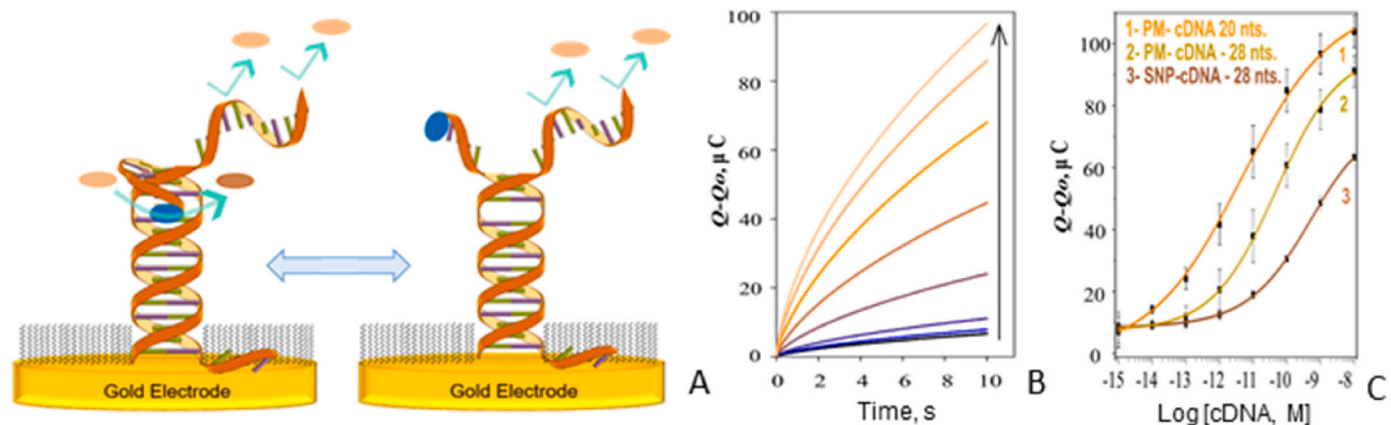
Fig. 3. (A) Schematic representation of the duplex formation at the electrodes, between the MB-labelled 20 nts hairpin ssDNA hybridized with 28 nts long cDNA. (B) Representative CC data recorded with ssDNA-modified Au SPE at −0.4 V in 20 mM PB/0.2 mM $K_3[Fe(CN)_6]$, in the presence of increasing concentrations of 28 nts PM-cDNA as indicated by arrow: 1, 10, 100 fM, 1, 10, 100 pM, 1 and 10 nM. (C) Calibration curves for (1) 20 nts PM-cDNA, (2) 28 nts PM-cDNA, and (3) 28 nts SNP-cDNA detection constructed with CC data. Γ_{MB}: 2.6 ± 2.0; 2.9 ± 0.1 and 2.8 ± 0.1 pmol cm^{-2}, respectively.

dropped down, and LOD increased to 10 fM, implying structurally impeded intercalation of MB into the formed duplex, now spaced from the duplex both by the alkane linker and 5 nts long stem-composing region. What is interesting, the signal from SNP-containing 28 nts long cDNA was eventually similar to that observed with its 20 nts analogue, due to the formation of the Y-shaped 10 nts duplexes when this SNP was present in both cDNA sequences (Papadakis et al., 2012) (Figs. 3C and 2D). The ability of duplex formation between the hairpin probe and SNP-containing 28 nts cDNA appeared to be very similar to that of 20 nts DNA (both have similar T_m), however, the ability of the MB label intercalation was improved compared to the perfectly matched duplex formed with 28 nts cDNA, due to the longer, and thus more flexible 10 nts spacer.

Electrocatalytic detection of E.coli rRNA. For detection of bacterial rRNA, the hairpin ssDNA probes with 6 and 7 nts introduced for the stem formation were designed that could recognize the 23S region of *E.coli* ribosomal RNA showed to be highly specific for *E. coli* (Khan et al., 2007). Two designed 27 nts and 28 nts beacons had alkanethiol

modifications introduced in either 3′ or 5′ end, correspondingly (Figs. S5 and SI). The T_m of the hairpin probes and formed duplexes was 42-37 °C and 53-52 °C, correspondingly, and approached those of the model beacon system. That ensured both the probe stability in its folded state, its hybridizability, and the possibility of duplex de-hybridization during sensor preparation. Both probes were used for CC detection of 22 nts long cDNA specific for 23S rRNA of *E. coli*, and both formed duplexes that had either 6 or 7 nts overhangs bearing the MB label (Fig. 4A, Figs. S5 and SI). DNA probe immobilization through the 3′ end generated a higher response to hybridization and the higher sensitivity of detection compared to the probe immobilized via its 5′end, which could be ascribed to different structural arrangements of 5′-tethered and 3′-tethered DNAs on the electrode surface, offering different hybridization patterns (Farjami et al., 2012). In further studies, 23S rRNA-specific probe immobilized on Au SPE via 3′ has been used for detection of rRNA isolated from *E.coli* cells.

The total RNA content extracted from *E. coli* cells was assayed directly using the electrocatalytic genosensor (Fig. 4B). The negative
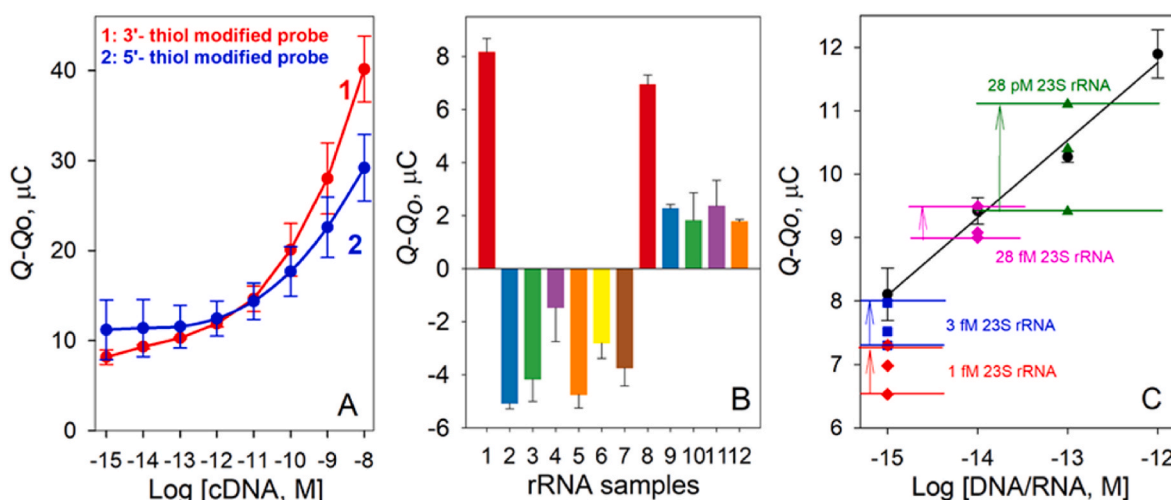
Fig. 4. (A) Calibration curves for *E.coli*-specific synthetic 22 nts *c*DNA constructed with CC data recorded at −0.4 V, in 20 mM PB/0.2 mM $K_3[Fe(CN)_6]$, with the Au SPE electrodes modified with *E.coli*-specific (1) 3′and (2) 5′-immobilized DNA probes, Γ_{MB}: 2.6 ± 0.1 and: 3.5 ± 0.2 pmol cm^{-2}; (B) Genosensor responses to (1) 1 fM synthetic cDNA, (2) 100 pM and (3) 100 fM total *E.coli* rRNA; (4) 100 pM and (5) 100 fM total *B. subtilis* rRNA; (6) 100 pM and (7) 100 fM total *P. fluorescens* rRNA; (8) 1 fM digested *E. coli* rRNA; (9) 27.5 pM and (10) 100 fM digested *B. subtilis* rRNA, and (11) 147.7 pM and (12) 100 fM digested *P. fluorescens* rRNA. (C) Response from the site-specifically digested 23S rRNA from *E. coli* plotted versus the synthetic DNA calibration curve. Analyzed concentrations of rRNA samples determined optically (SI): ca. 1 fM (15 CFU mL^{-1}), 3 fM (43 CFU mL^{-1}), 28 fM (337 CFU mL^{-1}), and 28 pM (337 × 10^3 CFU mL^{-1}) digested 23S rRNA. Each rRNA sample was analyzed in triplicates, each time with a freshly prepared electrode.

response was detected from 100 fM to 100 pM total *E. coli* rRNA, consistent with the restricted availability of the *E.coli*-specific region of 2904 nts long 23S rRNA sequence for hybridization (Ludwig and Schleifer, 1994) and partial fouling of the electrode surface by the negatively-charged rRNA, impeding the residual discharge of ferricyanide. Negative responses were also observed with total rRNA samples extracted from *B. subtilis* and *P. fluorescens* cells, also consistent with a surface fouling with rRNA (Fig. 4B).

To facilitate detection and avoid complications associated with the targeted rRNA sequence accessibility, *E. coli*-specific sequence region was enzymatically cut out of the whole 23S rRNA sequence by the RNase H enzyme, and such digested rRNA was analyzed. Samples were not otherwise pre-treated, simulating the situation of the in-field detection. Different concentrations of enzymatically cleaved 23S rRNA produced CC signals that could be correlated with the synthetic cDNA calibration plot (Fig. 4C). The 1 to 3 fM digested *E.coli* rRNA samples produced responses slightly lower yet comparable with signals from 1 fM synthetic cDNA, while signals from the 28 fM digested rRNA sample fitted the 6 to 14 fM concentration range. The CC responses produced by 1–28 fM digested rRNA fitted concentrations slightly lower than optically detected yet of the same order of magnitude. Increasing the rRNA concentration to 28 pM (equivalent of 337×10^3 CFU mL^{-1}) produced, however, significantly, 3 orders of magnitude lower responses, fitting the 13 to 31 fM concentration range and demonstrating strong matrix effects due to the electrode fouling with the total rRNA (consider Fig. 4B, bars 2–7). The detected femtomolar *E. coli* 23S rRNA correlated with from 15 to 337 CFU mL^{-1} *E. coli* detection, which are challenging levels sought in food and dairy product analysis (Grade A Pasteurized Milk Ordinance, 2017). Therewith, pM and higher rRNA concentrations or the corresponding cell content can be easily detected with the existing ELISA or polymerase chain reaction protocols, enabling overall from 10^4 to 10^5 CFU mL^{-1} and from 10^3 to 10^4 CFU mL^{-1} LODs (Law et al., 2015; Wang and Salazar, 2016).

It is interesting that *B. subtilis* and *P. fluorescens* rRNA samples treated similarly to *E. coli* rRNA with P1/P2 and the digestion enzyme produced significant signals, though well below the LOD (Fig. 4B, bars 9–12). The RNase H reaction buffer used here contained a small amount of DTT as a reducing agent (see Experimental), which is a well-known displacement agent used both for replacing gold-bound species (proteins and thiolated compounds) (Tsai et al., 2012) and SAM formation on gold (Liang et al., 2018). Though the DTT concentration in final samples was around μM, it was still sufficient for partial removal of the original DNA SAM components resulting in SAM restructuring. Nevertheless, the DTT presence did not significantly interfere with *E.coli* 23S rRNA detection, but addressed slightly lower than expected signals from 1 fM – 28 fM digested *E. coli* rRNA, due to some DNA/mercaptohexanol removal, both decreasing the electrocatalytic response to additions of digested *E. coli* rRNA.

Thus, the electrocatalytic detection of bacterial rRNA is possible using Au SPE modified with the hairpin DNA probes, which allowed fast, 20 min immediate detection of *E.coli*-specific rRNA (or from other sources, once the probe sequences are correspondingly designed). The approach rivals most of the existing detection schemes (Table S1), and only enzyme-linked sandwich assays on magnetic beads show better aM performance in detecting bacterial rRNA, both due to sample pre-concentration and magnetic separation (Fapyane et al., 2018; Shipovskov et al., 2012).

4. Conclusions

Here, a fast and fM sensitive electrocatalytic "off-on" biosensing platform utilizing MB-labelled hairpin DNA beacons immobilized on Au screen printed electrodes was developed and applied for fM analysis of bacterial rRNA. Electrocatalysis of ferricyanide reduction by MB intercalating into the DNA duplexes, formed after 20 min hybridization of the hairpin probes with the target DNA in sampled solutions, allowed 1 fM detection of cDNA, enzymatically digested 23S rRNA in the total RNA content extracted from *E. coli* without any amplification and interference from non-specific RNA within just 20 min. The proposed assay is simple, ultrasensitive and highly robust due to the MB-labelled hairpin probes providing the minimized yet robust background signal. The suggested methodology can be extended to sensitive and selective fM analysis of any nucleic acids in excessive amounts of structurally related sequences, and be further adapted for microfluidic high throughput screening devices.

Declaration of competing interest

The authors declare that they have no known competing financial interests or personal relationships that could have appeared to influence the work reported in this paper.

Data availability

Data will be made available on request.

Appendix A. Supplementary data

Supplementary data to this article can be found online at https://doi.org/10.1016/j.bios.2023.115214.

References

Abi, A., Ferapontova, E.E., 2013. Electroanalysis of single-nucleotide polymorphism by hairpin DNA architectures. Anal. Bioanal. Chem. 405, 3693–3703.
Anson, F.C., 1966. Innovations in the study of adsorbed reactants by chronocoulometry. Anal. Chem. 38, 54–57.
Bonnet, G., Tyagi, S., Libchaber, A., Kramer, F.R., 1999. Thermodynamic basis of the enhanced specificity of structured DNA probes. Proc. Natl. Acad. Sci. U.S.A. 96, 6171.
Boon, E.M., Ceres, D.M., Drummond, T.G., Hill, M.G., Barton, J.K., 2000. Mutation detection by electrocatalysis at DNA-modified electrodes. Nat. Biotechnol. 18, 1096–1100.
Boon, E.M., Barton, J.K., Bhagat, V., Nersissian, M., Wang, W., Hill, M.G., 2003. Reduction of ferricyanide by methylene blue at a DNA-modified rotating-disk electrode. Langmuir 19, 9255–9259.
Campos, R., Kotlyar, A., Ferapontova, E.E., 2014. DNA-mediated electron transfer in DNA duplexes tethered to gold electrodes via phosphorothioated dA tags. Langmuir 30, 11853–11857.
Campos, R., Kékedy-Nagy, L., She, Z., Sodhi, R., Kraatz, H.-B., Ferapontova, E.E., 2018. Electron transfer in spacer-free DNA duplexes tethered to gold via dA$_{10}$ tags. Langmuir 34, 8472–8479.
Campuzano, S., Yáñez-Sedeño, P., Pingarrón, J.M., 2017. Electrochemical biosensing for the diagnosis of viral infections and tropical diseases. Chemelectrochem 4, 753–777.
Díaz-Fernández, A., Ferapontova, E.E., 2022. Covalent Hemin/G4 complex-linked sandwich bioassay on magnetic beads for femtomolar HER-2/neu detection in human serum via direct electrocatalytic reduction of oxygen. Anal. Chim. Acta 1219, 340049.
Fan, C., Plaxco, K.W., Heeger, A.J., 2003. Electrochemical interrogation of conformational changes as a reagentless method for the sequence-specific detection of DNA. Proc. Natl. Acad. Sci. U.S.A. 100, 9134–9137.
Fapyane, D., Nielsen, J.S., Ferapontova, E.E., 2018. Electrochemical enzyme-linked sandwich assay with a cellulase label for ultrasensitive analysis of synthetic DNA and cell-isolated RNA. ACS Sens. 3, 2104–2111.
Farjami, E., Clima, L., Gothelf, K., Ferapontova, E.E., 2011. "Off–On" electrochemical hairpin-DNA-based genosensor for cancer diagnostics. Anal. Chem. 83, 1594–1602.
Farjami, E., Campos, R., Ferapontova, E.E., 2012. Effect of the DNA end of tethering to electrodes on electron transfer in methylene blue-labeled DNA duplexes. Langmuir 28, 16218–16226.
Ferapontova, E., 2017a. Basic concepts and recent advances in electrochemical analysis of nucleic acids. Curr. Opin. Electrochem. 5, 218–225.
Ferapontova, E., 2017b. Hybridization biosensors relying on electrical properties of nucleic acids. Electroanalysis 29, 6–13.
Ferapontova, E.E., 2017c. Basic concepts and recent advances in electrochemical analysis of nucleic acids. Curr. Opin. Electrochem. 5, 218–225.

Ferapontova, E.E., 2020. Electrochemical assays for microbial analysis: how far they are from solving microbiota and microbiome challenges. Curr. Opin. Electrochem. 19, 153–161.

Ferapontova, E.E., Gothelf, K.V., 2009. Optimization of the electrochemical RNA-aptamer based biosensor for theophylline by using a Methylene Blue redox label. Electroanalysis 21, 1261–1266.

Furst, A.L., Hill, M.G., Barton, J.K., 2014. Electrocatalysis in DNA sensors. Poylhedron 84, 150–159.

Furst, A.L., Muren, N., Hill, M.G., 2019. Toward multimarker and functional assays from crude cell lysates: controlling spacing and signal amplification in DNA-CT–based bioelectrochemical devices. Curr. Opin. Electrochem. 14, 104–112.

Garrido-Sanz, D., Redondo-Nieto, M., Martin, M., Rivilla, R., 2021. Comparative genomics of the Pseudomonas corrugata subgroup reveals high species diversity and allows the description of *Pseudomonas ogarae* sp. nov. Microb. Genom. 7, 000593.

Gómez-Arconada, L., Díaz-Fernández, A., Ferapontova, E.E., 2022. Ultrasensitive disposable apatasensor for reagentless electrocatalytic detection of thrombin: an O_2-Dependent hemin-G4-aptamer assay on gold screen-printed electrodes. Talanta 245, 123456.

Grade "A" Pasteurized Milk Ordinance, 2017. U.S. Department of Health and Human Services. Public Health Service and Food and Drug Admin.

Hartwich, G., Caruana, D.J., de Lumley-Woodyear, T., Wu, Y., Campbell, C.N., Heller, A., 1999. Electrochemical study of electron transfer through thin DNA films. J. Am. Chem. Soc. 121, 10803–10812.

Ingrosso, C., Corricelli, M., Bettazzi, F., Konstantinidou, E., Bianco, G.V., Depalo, N., Striccoli, M., Agostiano, A., Curri, M.L., Palchetti, I., 2019. Au nanoparticle in situ decorated RGO nanocomposites for highly sensitive electrochemical genosensors. J. Mater. Chem. B 7, 768–777.

Jamal, R.B., Shipovskov, S., Ferapontova, E.E., 2020. Electrochemical immuno- and aptamer-based assays for bacteria: pros and cons over traditional detection schemes. Sensors 20, 5561.

Jiang, T., Minunni, M., Wilson, P., Zhang, J., Turner, A.P.F., Mascini, M., 2005. Detection of TP53 mutation using a portable surface plasmon resonance DNA-based biosensor. Biosens. Bioelectron. 20, 1939–1945.

Kékedy-Nagy, L., Ferapontova, E.E., 2019. Directional preference of DNA-mediated electron transfer in gold-tethered DNA duplexes: is DNA a molecular rectifier? Angew. Chem. Int. Ed. 58, 3048–3052.

Kékedy-Nagy, L., Shipovskov, S., Ferapontova, E.E., 2016. Effect of a dual charge on the DNA-conjugated redox probe on DNA sensing by short hairpin beacon tethered to gold electrodes. Anal. Chem. 88, 7984–7990.

Kékedy-Nagy, L., Sørensen, K.D., Ferapontova, E.E., 2018. Picomolar sensitive and SNP-selective "Off-On" hairpin genosensor based on structure-tunable redox indicator signals. Biosens. Bioelectron. 117, 444–449.

Kékedy-Nagy, L., Shipovskov, S., Ferapontova, E.E., 2019. Electrocatalysis of ferricyanide reduction mediated by electron transfer through the DNA duplex: kinetic analysis by thin layer voltammetry. Electrochim. Acta 318, 703–710.

Kelley, S.O., Boon, E.M., Barton, J.K., Jackson, N.M., Hill, M.G., 1999. Single-base mismatch detection based on charge transduction through DNA. Nucleic Acids Res. 27, 4830–4837.

Khan, I.U.H., Gannon, V., Kent, R., Koning, W., Lapen, D.R., Miller, J., Neumann, N., Phillips, R., Robertson, W., Topp, E., van Bochove, E., Edge, T.A., 2007. Development of a rapid quantitative PCR assay for direct detection and quantification of culturable and non-culturable Escherichia coli from agriculture watersheds. J. Microbiol. Methods 69, 480–488.

Khater, M., de la Escosura-Muñiz, A., Quesada-González, D., Merkoçi, A., 2019. Electrochemical detection of plant virus using gold nanoparticle-modified electrodes. Anal. Chim. Acta 1046, 123–131.

Kirsch, J., Siltanen, C., Zhou, Q., Revzin, A., Simonian, A., 2013. Biosensor technology: recent advances in threat agent detection and medicine. Chem. Soc. Rev. 42, 8733–8768.

Kjällman, T.H.M., Peng, H., Soeller, C., Travas-Sejdic, J., 2008. Effect of probe density and hybridization temperature on the response of an electrochemical hairpin-DNA sensor. Anal. Chem. 80, 9460–9466.

Koo, K.M., Carrascosa, L.G., Shiddiky, M.J.A., Trau, M., 2016. Amplification-free detection of gene fusions in prostate cancer urinary samples using mRNA–gold affinity interactions. Anal. Chem. 88, 6781–6788.

Lai, R.Y., Lagally, E.T., Lee, S.-H., Soh, H.T., Plaxco, K.W., Heeger, A.J., 2006. Rapid, sequence-specific detection of unpurified PCR amplicons via a reusable, electrochemical sensor. Proc. Natl. Acad. Sci. U.S.A. 103, 4017–4021.

Laviron, E., 1979. General expression of the linear potential sweep voltammogram in the case of diffusionless electrochemical systems. J. Electroanal. Chem. 101, 19–28.

Law, J.W.-F., Ab Mutalib, N.-S., Chan, K.-G., Lee, L.-H., 2015. Rapid methods for the detection of foodborne bacterial pathogens: principles, applications, advantages and limitations. Front. Microbiol. 5 (770).

Liang, P., Canoura, J., Yu, H., Alkhamis, O., Xiao, Y., 2018. Dithiothreitol-regulated coverage of oligonucleotide-modified gold nanoparticles to achieve optimized biosensor performance. ACS Appl. Mater. Interfaces 10, 4233–4242.

Liu, G., Wan, Y., Gau, V., Zhang, J., Wang, L., Song, S., Fan, C., 2008. An enzyme-based E-DNA sensor for sequence-specific detection of femtomolar DNA targets. J. Am. Chem. Soc. 130, 6820–6825.

Liu, J., Yuan, X., Gao, Q., Qi, H., Zhang, C., 2012. Ultrasensitive DNA detection based on coulometric measurement of enzymatic silver deposition on gold nanoparticle-modified screen-printed carbon electrode. Sensor. Actuator. B Chem. 162, 384–390.

Lubin, A.A., Lai, R.Y., Baker, B.R., Heeger, A.J., Plaxco, K.W., 2006. Sequence-specific, electronic detection of oligonucleotides in blood, soil, and foodstuffs with the reagentless, reusable E-DNA sensor. Anal. Chem. 78, 5671–5677.

Ludwig, W., Schleifer, K.H., 1994. Bacterial phylogeny based on 16S and 23S rRNA sequence analysis. FEMS Microbiol. Rev. 15, 155–173.

Malecka, K., Ferapontova, E.E., 2021. Femtomolar detection of thrombin in serum and cerebrospinal fluid via direct electrocatalysis of oxygen reduction by the covalent G4-hemin-aptamer complex. ACS Appl. Mater. Interfaces 13, 37979–37988.

Malecka, K., Stachyra, A., Góra-Sochacka, A., Sirko, A., Zagórski-Ostoja, W., Radecka, H., Radecki, J., 2016. Electrochemical genosensor based on disc and screen printed gold electrodes for detection of specific DNA and RNA sequences derived from Avian Influenza Virus H5N1. Sensor. Actuator. B Chem. 224, 290–297.

Palecek, E., Bartosik, M., 2012. Electrochemistry of nucleic acids. Chem. Rev. 112, 3427–3481.

Papadakis, G., Tsortos, A., Bender, F., Ferapontova, E., Gizeli, E., 2012. Direct detection of DNA conformation in hybridization processes. Anal. Chem. 84, 1854–1861.

Piana, S., Bilic, A., 2006. The nature of the adsorption of nucleobases on the gold [111] surface. J. Phys. Chem. B 110, 23467–23471.

Ricci, F., Lai, R.Y., Heeger, A.J., Plaxco, K.W., Sumner, J.J., 2007. Effect of molecular crowding on the response of an electrochemical DNA sensor. Langmuir 23, 6827–6834.

Rossetti, M., Brannetti, S., Mocenigo, M., Marini, B., Ippodrino, R., Porchetta, A., 2020. Harnessing effective molarity to design an electrochemical DNA-based platform for clinically relevant antibody detection. Angew. Chem. Int. Ed. 59, 14973–14978.

Shipovskov, S., Saunders, A.M., Nielsen, J.S., Hansen, M.H., Gothelf, K.V., Ferapontova, E.E., 2012. Electrochemical sandwich assay for attomole analysis of DNA and RNA from beer spoilage bacteria Lactobacillus brevis. Biosens. Bioelectron. 37, 99–106.

Slinker, J.D., Muren, N.B., Renfrew, S.E., Barton, J.K., 2011. DNA charge transport over 34 nm. Nat. Chem. 3, 228–233.

Trasatti, S., Petrii, O.A., 1992. Real surface area measurements in electrochemistry. J. Electroanal. Chem. 327, 353–376.

Tsai, D.-H., Shelton, M.P., DelRio, F.W., Elzey, S., Guha, S., Zachariah, M.R., Hackley, V. A., 2012. Quantifying dithiothreitol displacement of functional ligands from gold nanoparticles. Anal. Bioanal. Chem. 404, 3015–3023.

Wang, Y., Salazar, J.K., 2016. Culture-independent rapid detection methods for bacterial pathogens and toxins in food matrices. Compr. Rev. Food Sci. Food Saf. 15, 183–205.

Who, 1997. Surveillance and Control of Community Supplies. Guidelines for drinking -water quality, Geneva.

Xiao, Y., Lubin, A.A., Baker, B.R., Plaxco, K.W., Heeger, A.J., 2006. Single-step electronic detection of femtomolar DNA by target-induced strand displacement in an electrode-bound duplex. Proc. Natl. Acad. Sci. USA 103, 16677.

Xiao, Y., Lai, R.Y., Plaxco, K.W., 2007a. Preparation of electrode-immobilized, redox-modified oligonucleotides for electrochemical DNA and aptamer-based sensing. Nat. Protoc. 2, 2875–2880.

Xiao, Y., Qu, X., Plaxco, K.W., Heeger, A.J., 2007b. Label-free electrochemical detection of DNA in blood serum via target-induced resolution of an electrode-bound DNA pseudoknot. J. Am. Chem. Soc. 129, 11896–11897.

Xiao, Y., Lou, X., Uzawa, T., Plakos, K.J.I., Plaxco, K.W., Soh, H.T., 2009. An electrochemical sensor for single nucleotide polymorphism detection in serum based on a triple-stem DNA probe. J. Am. Chem. Soc. 131, 15311–15316.